UNIVERSITY OF OKLAHOMA

GRADUATE COLLEGE

COMPARATIVE ANALYSIS OF USER-CELL ASSOCIATION METHODS FOR MILIMETER WAVE MASSIVE MIMO BY DEVELOPING A SYSTEM LEVEL SIMULATOR FOR HETNETS

A THESIS

SUBMITTED TO THE GRADUATE FACULTY

in partial fulfillment of the requirements for the

Degree of

MASTER OF SCIENCE IN TELECOMMUNICATIONS ENGINEERING

By

SINASI CETINKAYA
Norman, Oklahoma
2017

COMPARITIVE ANALYSIS OF USER-CELL ASSOCIATION METHODS FOR MILIMETER WAVE MASSIVE MIMO BY DEVELOPING A SYSTEM LEVEL SIMULATOR FOR HETNETS

A THESIS APPROVED FOR THE
SCHOOL OF ELECTRICAL AND COMPUTER ENGINEERING

BY

Dr. Ali Imran, Chair

Dr. Pramode Verma

Dr. Kam Wai Clifford Chan

This master's thesis is dedicated to my beloved family who always encouraged me and believed in me and all teachers I have had my whole life.

Acknowledgements

I gratefully acknowledge the support and guidance of the everyone in TCOM family at the University of Oklahoma. Most particularly, I owe a debt of gratitude to my academic advisor Dr. Ali Imran for his help, continuous guidance and encouragement. I am very thankful to him for giving his valuable time to discuss the issues related to my thesis work, which helped me understand my mistakes and obtain fruitful results regarding my thesis. I again thank him for letting me study with an expert like him in his research area. Without his kind, thoughtful and wise supervision, I would have never been able to manage my time and finalize this work.

Next, I would like to express my sincere and deep gratitude to my committee members, Dr. Pramode Verma for letting me be a member of TCOM at the University of Oklahoma, the wise way he teaches, his kindness and encouragement, and Dr. Kam Wai Clifford Chan for his valuable guidance, suggestions and comments during the entire thesis research and writing process.

I would like to extend my thanks to Ms. Renee Wagenblatt and all my laboratory colleagues for their support and kind help in order to understand and be clear at every step of my thesis research. Especially, my deep gratitude goes to my seniors and valuable friends Ahmad Asghar and Hasan Farooq. I have learned a lot from them and I will always owe them during all my life.

My final appreciation and dedication of this work is for my family, since they are the reason for my success in this life. I am working and studying so far away from my family just to make them proud of my accomplishments. I want to emphasize that without them there is no meaning of anything in the world.

Table of Contents

List of Tables

List of Figures

Abstract

Massive multiple-input-multiple-output (MIMO) base station deployments and millimeter wave (mmWave) spectrum utilization have been identified as promising disruptive technologies, along with ultra-dense Heterogeneous Networks (UDHNs) to meet the exponential data requirement of the next generation cellular networks. With the proliferation of UDHNs, optimal user-cell association in cellular networks, which is a well-known open problem, will be exacerbated due to the power differential of macro and small cells. This study investigates the user-cell association problem for ultra-dense two-tier networks with massive MIMO deployment and small cells operating in mmWave spectrum. The association problem is modeled as a convex utility maximization problem, adapted from [11], and is a function of the user throughput. The problem is solved through a centralized subgradient algorithm. Additionally, a game theoretical user-centric distributed load balancing algorithm, inspired from [32], where each user chooses its serving base station to maximize its user throughput selfishly, is also evaluated. Moreover, these adapted algorithms are compared against smallest pathloss and maximum downlink data rate association methods and it is demonstrated via extensive simulations that both the centralized and user-centric approaches almost equally outperform the smallest pathloss and maximum downlink data rate association methodologies in terms of user throughput and cell load distribution. The results exhibit average throughput gains between 20% and 40% for the majority of users if massive MIMO UDHN deployments are operated in the mmWave spectrum as compared to existing sub-6 GHz bands under the optimal user-cell association schemes.

Chapter 1: Introduction

Ever-growing demand for higher data rate in mobile cellular networks due to rapidly developing technologies like device to device communication (D2D), small cell deployment, internet of things (IoT), HD video streaming and online applications such as e-banking have incited new methodologies to complement existing cellular technologies for data rate improvement. Three of the leading candidate methodologies for data rate improvement in future mobile cellular networks include deployment of large number of small cells, mmWave spectrum and massive MIMO systems. However, these technologies face several key challenges towards integration with existing and future cellular networks. These include resource allocation, user-cell association, efficient spectrum utilization, interference mitigation, and power consumption.

This thesis addresses the two key problems in a two-tier ultra-dense mmWave massive MIMO network: 1) The need for simulator supporting a very large number of antennas for mmWave massive MIMO systems in Heterogeneous Networks (HetNets), and 2) Investigation of user-cell association at mmWave frequency range.

1.1 mmWave Massive MIMO Ultra-Dense Heterogeneous Cellular Networks

The 21st century has already seen an exponential growth in wireless data usage, thanks to the high proliferation of smart devices and ever increasing mobile applications. With the introduction of new applications, such as augmented reality and IoT, this trend is expected to only grow further. For instance, a forecast by CISCO showed that the overall mobile data traffic is expected to increase from 2.5 EBs per month in 2014 to 24.3 EBs per month by 2019 [1]. The next generation of wireless networks, often referred to as "5G" is targeting a data capacity increase of (100-1000x) from the current 4G LTE networks [2]. Three design targets of next generation 5G wireless technology will involve utilization of ultra-dense networks, new available large amount of bandwidth in the mmWave spectrum, and higher spectral efficiency afforded by massive MIMO systems. This has motivated the most recent research interests towards the merger of mmWave spectrum and massive MIMO technology with the deployment of ultra-dense networks which is essentially known as small cell deployment.

Cell densification with different types of base stations (BSs) such as macro and small BSs with different transmit powers is a technique that already has been deployed in the current fourth generation (4G) cellular networks. This technique can boost the network capacity with high density deployment and offer user offloading from macro BSs to small BSs.

Additionally, massive MIMO and mmWave spectrum utilization have been identified as key enabling solutions to achieve more data capacity as envisioned for 5G. Massive MIMO is a multiuser MIMO technology where each BS is equipped with an array of hundreds of active antenna elements to communicate with single-antenna user terminals that are far less in number as compared to the antenna elements at the BS. On the other hand, given the shortage of available spectrum at traditional cellular frequencies, mmWave spectrum (30 GHz -300 GHz) can be utilized to increase the available spectrum by 200 times as compared to presently allocated sub 6 GHz spectrum [3]. Although mmWave spectrum was considered unsuitable for cellular communication in the past due to large free space pathloss and poor penetration through water and concrete walls, recent mmWave outdoor propagation measurements and channel modeling has revealed its promising potential for dense urban small cell deployments [4]. Furthermore, the smaller wavelengths at mmWave frequencies enable large antenna arrays and spatial beamforming techniques [5] which provide array gains to counter the larger free space attenuation.

Massive MIMO antenna arrays have smaller antenna form factors at mmWave frequency range making them suitable for dense urban deployment in a multi-tier network consisting of dense small BSs tier overlaying relatively sparsely deployed macro BSs. The deployment of large number of antennas at the base stations can provide a significant increment in the spectral and energy efficiency of the cellular networks - thanks to beamforming techniques [6]. Transmitting independent data streams simultaneously to multiple users sharing same transmission resources leads to higher spectral efficiency. In addition to that, very large array gain offered by massive MIMO enhances energy efficiency of network.

Deployment of mmWave frequency spectrum can meet demand for high data rate for indoor high-speed wireless applications and be very suitable candidate for outdoor point-to-point backhaul links. However, mmWave deployment is still being debated due to its limitations such as the very high free space pathloss in the first meter of propagation, rain fading, penetration loss and high oxygen (O_2) absorption due to higher frequencies. Nevertheless, these limitations can be overcome through dense deployment of small cells with hundreds of antennas which can provide very high capacity enhancement in conjunction with short-range mmWave technology. Figure 1 shows a potential 5G network architecture with high frequency (HF) and mmWave massive MIMO deployment. Figure 1 shows that operating at mmWave frequency can enable large number of antenna deployment even in some transportation systems, which have enough space for the deployment, for next generation 5G HetNets. Additionally, it is shown that 5G network architecture can operate at both HF and mmWave frequencies concurrently. In the Figure 1, fiber or wireless backhauls are used in order to coordinate BSs. Moreover, the 5G HetNet architecture can embody virtual cells which can be either user centric or network centric [7].

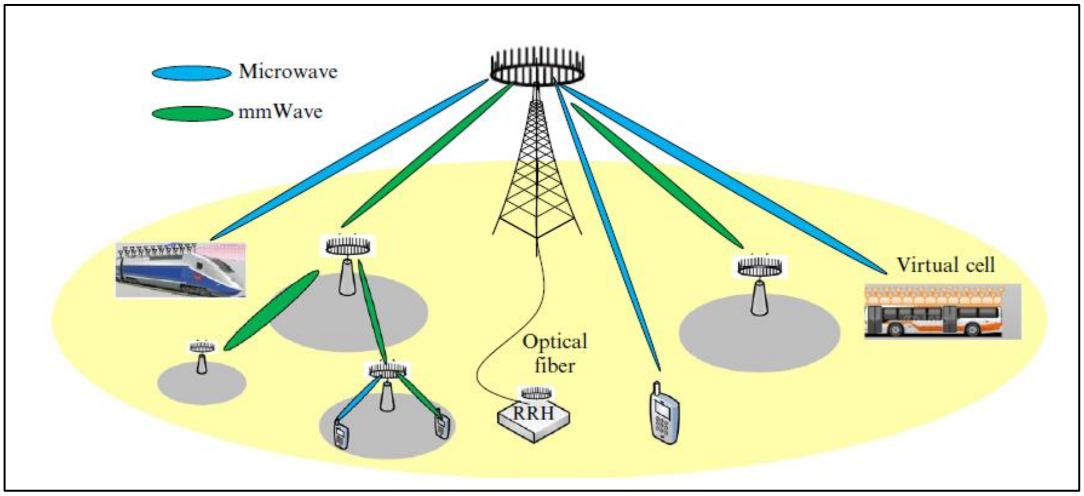

Figure 1. 5G network architecture with mmWave massive MIMO deployment

For HetNets with co-existing mmWave small BSs and sub 6 GHz macro BSs, the problem of inter-tier and intra-tier offloading becomes non-trivial and requires incorporating the impact of load on rate characterization [8]. Another associated challenge that has not been extensively researched so far is the optimal user-cell association particularly with mmWave small cells. Due to high sensitivity of the mmWave to static blockages such as buildings, a significantly high pathloss for non-line-of-sight (NLOS) mmWave links is experienced which results in significantly different pathloss exponents for line-of-sight (LOS) and NLOS scenarios [9]. Additionally, the abrupt nature of the mmWave channel renders Reference Signal Received Power (RSRP) and/or Reference Signal Received Quality (RSRQ) [10] as unsuitable candidates for the user-cell association criteria.

Recently several advanced user-cell association schemes have been proposed vis-à-vis massive MIMO deployment in HF spectrum [11], [12]. Given the contrasting beamforming designs and channel blockage effects, how well these association schemes work in a massive MIMO mmWave deployment at femto BSs and how much gain (if any) can be expected is yet to be explored. To the best of my knowledge, this thesis is first attempt to investigate this problem as this thesis has proposed.

1.2 Contributions

The contributions of this thesis are presented below:

- User-cell association in massive MIMO deployments in mmWave based UDHNs requires understanding and incorporation of mmWave specific channel characteristics as well as practical beamforming strategies for each tier in dense urban environments. Keeping these factors in consideration, this thesis offers a system model that enables a comparative analysis of the recently proposed optimal user-cell association schemes with the traditional approaches from the non-massive MIMO era.
- For the designed system model, a network utility function is defined as a function of user throughputs for optimal user-cell association and a logarithmic network utility maximization problem with proportional fairness between the users is formulated. It is shown that the network utility function is convex and achieves global optimum when unique user-cell association is employed, i.e. when each user is associated to one small

BS at maximum during any arbitrary time slot [11]. Contrary to the recently proposed approach in [11] which optimizes user-cell association based on per user instantaneous data rates, this thesis considers the effect of increased bandwidth available at mmWave spectrum in the utility function that enables higher data rates and consequently higher probability for user offloading from macro BS to small BS tier.

- In order to simulate massive MIMO UDHNs operating at mmWave spectrum, a system level LTE simulator has been developed as part of this study. The simulator, which has been adapted from an existing simplified LTE simulator, contains module which can calculate SINR value with conjugate beamforming, zero-forcing beamforming (ZFBF) and analog beamforming. Additionally, inter-cell interference and pilot contamination are also considered in this module. A module is also added to simulate massive MIMO and MIMO systems in the simulator. The simulator also incorporates mmWave pathloss model as well as two additional network topologies for UDHNs. The simulator also allows the option to choose from two different user-cell association algorithms adapted from [11] i.e., smallest pathloss and maximum downlink data rate algorithms.
- This thesis performs a comparative analysis of four different user-cell association methods by leveraging the mmWave massive MIMO system model. The results indicate superior performance of the centralized subgradient and distributed user-centric association as compared to the

traditional maximum downlink data rate and smallest pathloss association schemes. Additionally, performance comparison with the existing massive MIMO UDHNs model [11] reveals that operating the small BSs at higher frequency (mmWave) enables throughput gains due to higher spectrum availability and stronger pathloss degradation of the interfering signals.

1.3 Organization

This thesis is organized into four parts as follows: Chapter 2 details the problem of optimal user-cell association scheme for next generation ultra-dense mmWave massive MIMO cellular networks. In addition to that, radio propagation is also discussed in Chapter 2. Chapter 3 presents a new MATLAB based improved system level simulator developed as a part of this study to enable investigation of mmWave massive MIMO for heterogeneous networks. An analysis and comparison of the performance of algorithms, explained in Chapter 2, for the massive MIMO deployment in HF spectrum and mmWave spectrum is presented in Chapter 4. Finally, the thesis concludes with future prospects of this study in Chapter 5.

Chapter 2: User-Cell Association Methods for mmWave Massive MIMO Wireless Networks

In this chapter, Section 2.1 gives a brief survey of existing works for user-cell association and load balancing. The system model for mmWave massive MIMO UDHNs is described and a convex problem formulation adapted from [11] are given in Section 2.2. Additionally, the Langrangian dual analysis is studied for the user-cell association problem in Section 2.3. Finally, this chapter describes maximum downlink data rate method, smallest pathloss method and a game theoretical user-centric method for user-cell association in Section 2.4.

2.1 Related Works

Although user-cell association has been extensively discussed in literature, few studies have discussed it from the perspective of newly-emerging mmWave HetNets. In this section, the literature related to user-cell association and load balancing with the fairness criteria in multi-tier wireless networks has been reviewed. The section closes with a summary of the objective presented in the thesis.

In conventional networks, users are associated with the BSs that provide the highest received power [13]. However, this can cause macro BSs to become heavily loaded when heterogeneity is considered due to the different transmit powers of macro and small BSs. Therefore, a new user-cell association methodology is required for the efficient use of resources in the network. In case of massive MIMO UDHNs, maximum RSRP based association does not provide the same user association as that with maximum SINR based association. This is due to beamforming techniques which increase the SINR with respect to the number of transmit antennas. In this regard, in [14], it is shown that *biasing* can provide load balancing by increasing the coverage of small BSs with an artificial biasing value. This raises a new problem relating to the optimal biasing value. Similarly, [15] also considers a fixed bias value for user offloading to small cells. In [11], the optimal user-cell association is defined using a convex problem and the utility function is maximized by solving a centralized subgradient algorithm in massive MIMO UDHNs operating at HF spectrum. The load balancing is proposed for massive MIMO UDHNs in [11] by a game theoretical approach where each user tries to maximize their throughput in a selfish way. However, this work does not consider mmWave as this thesis does.

While one of the early studies in client association [16] aims to maximize network utility function under joint power constraints in downlink code-division multiple access (CDMA) networks, it is shown that joint optimization of client association can increase the overall network throughput. Network utility maximization is also considered in [17] with proportional fairness where scheduler allocates more RBs to a user who has better channel quality. Similar to the approach in [11], in [18], the authors propose a game theoretical algorithm for association problem and maximize the user throughput at the Nash equilibrium.

In [19], a dual subgradient based algorithm is proposed as a solution of network utility maximization problem in massive MIMO HetNets to maximize rate gain and minimize interference challenges originating from small cell deployment. The proposed algorithm provides more than 2x rate gain for cell edge users and optimal user-cell association without interference management. However, the mmWave spectrum has not been considered in this work.

In [20], optimal user-cell association in mmWave 60 GHz is considered. The authors propose a distributed algorithm to optimize the user-cell association by balancing BS utilization. Another study [21] proposes a network utility maximization problem with proportional fairness in mmWave massive MIMO HetNets. The low complexity distributed algorithm maximizes the network utility function under power constraints. According to the power constraints, the price of power consumption cannot be more than harvested energy. The proposed algorithm outperforms the maximum RSRP and maximum SINR schemes by providing higher throughput.

In this thesis, two algorithms are adapted from [11] with the additional difference of considering utility function as a function of bandwidth. However, in the proposed system model, the small BSs and macro BSs operates in different spectrum with different amount of bandwidth. Therefore, a convex network utility maximization problem in case of mmWave UDHNs is formulated and solved by a centralized subgradient algorithm. Additionally, the user throughput is maximized by a game theoretical user-centric distributed algorithm.

2.2 System Model

2.2.1 Radio Environment and Parameters

This thesis considers a two-tier system with macro BSs (MBSs) and small/femto BSs (FBSs) distributed across a 2-dimensional plane and operating in the HF and mmWave spectrum respectively. $j \in J$ = {MBS1, MBS2, ..., MBSM} U {FBS1, FBS2, ..., FBSF} and $k \in K$ = {1, 2, ..., K} are used to index the BSs (combination of M MBSs and F FBSs) and users respectively. The users are assumed to be distributed across the macro BS tier foot-prints in a non-homogenous manner with higher concentration within specified hotspots. The femto BS distribution is modeled using an independent Poisson Point Process. This work assumes that all users in the network are served with proportional fairness (PF) and each user is served by only one BS at a time. The notations used in this thesis are presented in Table 1.

Table 1 Notation Summary

Notation	Description
J, K	set of BSs (MBSs, FBSs), set of single antenna UEs
A_j	number of antennas at BS *j*
S_j	number of downlink data stream transmitted by BS *j* on a given slot
r_k	throughput of user *k*
$C_{k,j}$	downlink capacity of user *k* served by BS *j*
S_j/A_j	spatial load of BS *j*
$g_{k,j}$	pathloss and shadowing between BS *j* and user *k*
Q	number of symbols per slot for uplink pilots
T	number of downlink OFDM symbols per time slot
P_j	transmit power of BS *j*
d	distance between an arbitrary user and its associated BS
B	total bandwidth
N_0	noise power
N_F	noise figure
k_b	Boltzmann's constant
T_k	temperature in degrees Kelvin
$\lvert K_j \rvert$	number of users served by BS *j*
m_{i_k}	number of migrations observed by user *k* in *i*-th iteration
p	switching probability

This thesis assumes massive MIMO deployment both at macro BSs and femto BSs with A_j as the number of antennas and S_j as the data downlink stream capacity per time slot at any MBS / FBS *j*. Using time division multiplexing (TDD), the BSs learn about the channel coefficients via the pilots transmitted by the associated users in the uplink. This allows each BS to serve a set of up to S_j associated UEs within one time slot by using linear zero-forcing beamforming (LZFBF) and analog beamforming in MBS and FBS tiers respectively. The beamforming gain is particularly important for the mmWave channel to offset the free space pathloss due to higher frequency and blockage effect.

For transmission, this work considers OFDMA based scheme where each user schedules transmissions over contiguous time frequency slots, also referred to as resource blocks (RBs) [22]. The block-fading channel model that captures the effect of both large-scale and small-scale fading is assumed. The shadowing effect (large-scale fading) between an arbitrary BS j and user k is considered constant across all RBs. Because the HF and mmWave spectrum exhibit varying channel characteristics, distinct small-scale fading models for MBS - user and FBS - user channels are used. For the MBS-user link, the small-scale channel coefficients which are same within every OFDM RB, but not necessarily same across RBs, are modeled as Rayleigh fading coefficients. In case of FBS-user association, the small-scale channel is modeled by independent Nakagami fading for each channel with different coefficients N_L and N_N for LOS and NLOS links. If $h_{k,j}$ represents the small-scale fading between a user k and a FBS j, then $|h_{k,j}|^2$ is a normalized Gamma random variable. However, due to the effect of channel hardening in massive MIMO systems [23], the effect of small scale channel coefficients is ignored in the model, i.e., it is considered that $\left|h_{k,j}\right| = 1,\ \forall\ k\epsilon K, j\epsilon\ J$.

2.2.2 Blockage Model

In outdoor communication, blockages cause very different pathloss values for LOS and NLOS links [24]. mmWave signals not only have attenuation because of the high building but also they tend to attenuate due to smaller objects like human body. In order to model pathloss in mmWave frequency, there is a need for a blockage model to calculate pathloss values with higher accuracy and in a more realistic manner. Therefore, a blockage model suggested by 3GPP to differentiate between LOS and NLOS link is assumed. The model suggested in 3GPP [25], [26] is given in Figure 2.

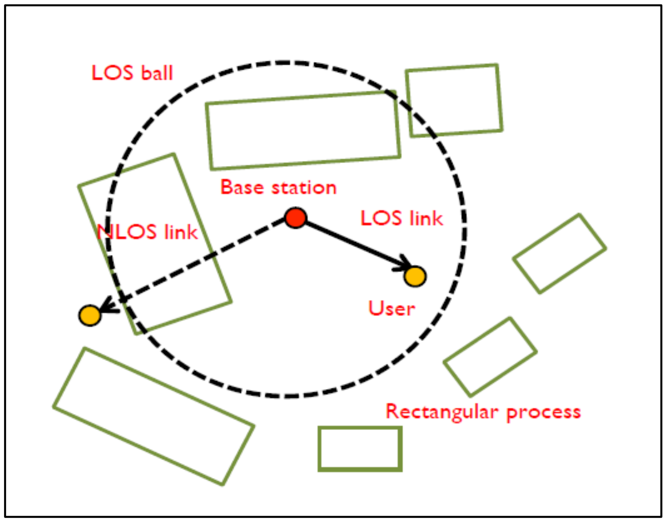

Figure 2. Building blockages model

The model calculates a distance dependent probability function. Although the function is dependent on the distance, it is a deterministic non-increasing function of distance and can take values between 0 and 1 only. The function makes a mapping based on the distance and calculates assuming it is LOS. Even though the function $P_{LOS}(d)$ is dependent on distance, it can vary for different environments like urban and suburban areas. This work assumes an urban scenario and the function [26] is given for urban areas below.

$$P_{LOS}(d) = \min\left(\frac{18}{d}, 1\right)\left(1 - e^{-\frac{d}{63}}\right) + e^{-\frac{d}{63}} \tag{1}$$

The function calculates a LOS probability based on a LOS region for a user k determined according to the position of nearby buildings like in Figure 2.

2.2.3 *Downlink capacity and user throughput in mmWave massive MIMO systems*

The instantaneous downlink capacity within one time slot is given by the logarithm of one plus the signal-to-interference-plus-noise ratio (SINR). The throughput introduced in [27], which is the downlink capacity in unit of bps, includes the total bandwidth, the ratio of number of symbols used sending data to the total number of resource blocks which are 7 OFDM symbol long, and the ratio of useful symbol duration to the OFDM symbol interval:

$$C_{k,j} = B\left(\frac{T-Q}{T}\right)\left(\frac{T_u}{T_s}\right)\log_2(1 + SINR_{k,j}) \quad (2)$$

where B is the total bandwidth, Q is the number of symbols per slot for uplink pilots and T is the total number of OFDM symbols within each time slot. $\frac{T_u}{T_s}$ is the ratio of useful symbol duration to the total symbol duration and has been considered as unity without any loss of generality.

Let $u_{k,j}$ be and index indicating that an arbitrary user k is connected to a BS j, then

$$u_{k,j} = \begin{cases} 1, \text{if user } k \text{ associated with BS } j \\ 0, \text{otherwise} \end{cases} \quad (3)$$

The load of BS j in a given time slot is assumed as the number of users associated with it which can be expressed by

$$|K_j| = \sum_{k \epsilon K} u_{k,j}, \forall\, j \epsilon J \quad (4)$$

The user throughput adapted from [11] is given as:

$$r_{k,j} = \sum_{j \epsilon J} \alpha_{k,j}\, C_{k,j}\ , \ \forall\, k \epsilon K \quad (5)$$

where $\alpha_{k,j}$ represents the activity fraction of RBs allocated to user k by the serving BS j, and can take value in the range [0,1].

$$\alpha_{k,j} = \begin{cases} \frac{S_j}{|K_j|}, \ \forall \ k\epsilon K_j \ if \ S_j \leq |K_j| \\ 1, \ \forall \ k\epsilon K_j \ if \ S_j \geq |K_j| \end{cases} \tag{6}$$

Note: *In this thesis, the terms capacity and rate are used interchangeably.*

2.2.4 User SINR with LZFBF

The achievable rate depends on the SINR value at a user *k* who is associated with BS j. It is assumed that perfect channel state information (CSI) is available. Under this assumption the SINR value at user *k* associated with a macro BS *j* is adapted from [28] and given by

$$SINR_{k,j} = \frac{(\frac{A_j}{S_j}-1)g_{k,j}^2 P_j}{\eta N_0 + \sum_{l\epsilon J:l\neq j} g_{k,l} P_l + \sum_{l\epsilon J(q(k)):l\neq j} (\frac{A_l}{S_l}-1) g_{k,l}^2 P_l} \tag{7}$$

In (7), $\eta \geq 1$ is the normalizing factor that guarantees that no BS infringes power constraints and the value of the normalizing factor is negligible when the number of antennas at BS j (A_j) is very large [27]. $g_{k,j}$ denotes the shadowing (large-scale) and distance dependent pathloss.

If the system is purely interference limited, the SINR value is dependent on the square of ($g_{k,j}$) which includes shadowing and pathloss [27]. Because of that, the SINR formula given above includes the square of $g_{k,j}$ on both the desired signal and inter-cell interference and the system noise power is given by $N_0 = N_F k_b T_k B$.

2.2.5 User SINR with analog beamforming

mmWave frequencies can reduce the physical size of the antenna arrays. This makes it possible to pack large number of antennas in a small area. When the number of antennas increases, the implementation of digital beamforming techniques like LZFBF becomes infeasible because of the higher power consumption and higher costs [29].

Therefore, the SINR value at user *k* associated with a femto BS *j* derived from [21], [27] is given by

$$SINR_{k,j} = \frac{(\frac{A_j}{S_j})g_{k,j}^2 P_j}{\eta N_0 + \sum_{l\epsilon J: l\neq j} G_l g_{k,l} P_l + \sum_{l\epsilon J(q(k)): l\neq j} (\frac{A_l}{S_l}) g_{k,j}^2 P_l} \tag{8}$$

where G_l expresses the relative power radiated by the interfering BS l in the direction of the user *k* served by BS *j* [21].

$$G_l = \begin{cases} \frac{A_l}{S_l}, & with\ probability\ \frac{1}{\sqrt{A_l}} \\ \frac{1}{sin^2\left(\frac{3\pi}{2\sqrt{\frac{A_l}{S_l}}}\right)}, & with\ probability\ \left(1 - \frac{1}{\sqrt{A_l}}\right) \end{cases} \tag{9}$$

mmWave systems are not interference limited but noise limited. In denominator of SINR equation, the effect of interference is negligible due to the high pathloss.

2.2.6 Convex Problem Formulation

This thesis assumes PF in the problem formulation in order to allocate more RBs to users with stronger downlink channels. A convex problem formulation is adapted from [11] with only an additional difference which is the definition of throughput. In [11], the throughput is given as a function of instantaneous rate, downlink data stream, and load of the BS. It does not consider bandwidth since both femto cells and macro cells operate at same HF and the total bandwidth is same both for femto cells and macro cells. However, in this work, macro and small cells operate at different frequencies and they both have different bandwidth. This makes the throughput function defined in [11] unadaptable. Therefore, the throughput function is considered as a function of bandwidth in this thesis.

In this regard, a logarithmic overall network utility function is defined as $U(\mathbf{r}) = \sum_k \log r_k$ which is maximum when the user throughputs are maximum. The given utility function is a concave and monotonically increasing. The following optimization problem manifests a logarithmic utility function for the optimal user-cell association for load balancing:

$$\underset{\boldsymbol{\alpha},\boldsymbol{r} \geq 0}{\text{maximize}}\, U(\mathbf{r}) \tag{10a}$$

$$\text{subject to } r_k \leq \sum_{j\epsilon J} \alpha_{k,j}\, C_{k,j}\ , \forall\ k\epsilon K \tag{10b}$$

$$\sum_{k\epsilon K} \alpha_{k,j} \leq S_j,\ \ \forall j\epsilon J \tag{10c}$$

$$\sum_{j\epsilon J} \alpha_{k,j} \leq 1, \quad \forall k\epsilon K \tag{10d}$$

$$r_k \geq 0, \alpha_{k,j} \geq 0, \forall k\epsilon K, j\epsilon J \tag{10e}$$

The constraint (10c) in the maximization framework limits the total activities of the users attached to BS *j* to be within the downlink data streams S_j. Similarly, constraint (10d) states that in case of multiple BS associations to a single user, the limit of the sum of activities of the all the BSs which serve a user *k* cannot exceed unity. Note that (10d) makes the problem (10) different from the classical unique association problem formulation, in which each user can only be served by one BS at max. However, the solution of (10) gives a feasible upper bound benchmark to any user-cell association which enforces unique association [11]. Finally, constraint (10e) ensures that no user is suffering from zero throughput, i.e. all admitted users have positive downlink data rates. The defined user association problem (10) is known to be convex with the solution providing an optimally feasible association configuration [11].

2.3 Langrangian Dual Analysis and Centralized Subgradient Algorithm Based Solution

For the solution of problem (10), the Langrangian duality function is given similar to [11] and it takes the form:

$$L(\boldsymbol{\alpha}, \boldsymbol{r}, \boldsymbol{\omega}, \boldsymbol{\mu}, \boldsymbol{\vartheta}) = U(\boldsymbol{r}) - \sum_k \omega_k \big(r_k - \sum_j \alpha_{k,j} C_{k,j}\big)$$

$$- \sum_j \mu_j \big(\sum_k \alpha_{k,j} - S_j\big) - \sum_k \vartheta_k \big(\sum_j \alpha_{k,j} - 1\big) \quad (11)$$

$$= U(\boldsymbol{r}) - \sum_k \omega_k r_k + \sum_j \mu_j S_j + \sum_k \vartheta_k + \sum_{(k,j)} \alpha_{k,j} (\omega_k C_{k,j} - \mu_j - \vartheta_k) \quad (12)$$

where $\boldsymbol{r} \geq 0$ and $\boldsymbol{\alpha} \geq 0$ are the primal variables and $\boldsymbol{\omega}, \boldsymbol{\mu}, \boldsymbol{\vartheta}$ are the Lagrange multipliers. The dual function G is the maximum of Langrangian function over $\boldsymbol{\alpha}$ and $\boldsymbol{r}$ and can be minimized over the feasible set of dual variables to give the optimal global solution of the convex problem (10).

$$G(\boldsymbol{\omega}, \boldsymbol{\mu}, \boldsymbol{\vartheta}) = \max_{\boldsymbol{\alpha}, \boldsymbol{r} \geq 0} L(\boldsymbol{\alpha}, \boldsymbol{r}, \boldsymbol{\omega}, \boldsymbol{\mu}, \boldsymbol{\vartheta}) \quad (13)$$

$$\text{minimize } G(\boldsymbol{\omega}, \boldsymbol{\mu}, \boldsymbol{\vartheta}) \quad (14a)$$

$$\text{subject to } \boldsymbol{\omega}, \boldsymbol{\mu}, \boldsymbol{\vartheta} \geq 0 \quad (14b)$$

The Langrangian dual function can be maximized when the term $\sum_{(k,j)} \alpha_{k,j} (\omega_k C_{k,j} - \mu_j - \vartheta_k)$ disappears. In this case, the dual function is modified as follow:

$$\text{minimize } \max_{\boldsymbol{r} \geq 0} \{ U(\boldsymbol{r}) - \sum_k \omega_k r_k \} + \sum_j \mu_j S_j + \sum_k \vartheta_k \quad (15a)$$

$$\text{subject to } \omega_k C_{k,j} \leq \mu_j + \vartheta_k, \forall\ (k, j) \quad (15b)$$

$$\boldsymbol{\omega}, \boldsymbol{\mu}, \boldsymbol{\vartheta} \geq 0 \quad (15c)$$

The term $\{ U(\boldsymbol{r}) - \sum_k \omega_k r_k \}$ can be written as $\{ \sum_k U(r_k) - \sum_k \omega_k r_k \}$, where $U(r_k) = \log(r_k)$ and it can be maximized individually. In this case, the maximum of this term is found at $r_k = \frac{1}{\omega_k}$ and the maximum value is $-\log(r_k) - 1$. From (15b), the dual variable ω_k can be eliminated, since the minimization over $\boldsymbol{\omega}$ can be found when $\omega_k = \min_j \left\{ \frac{\mu_j + \vartheta_k}{C_{k,j}} \right\}$. Finally, the dual function can be written as:

$$\min \sum_j \mu_j S_j + \sum_k \vartheta_k - \sum_k \log\Big(\min_j \left\{ \frac{\mu_j + \vartheta_k}{C_{k,j}} \right\} \Big) \quad (16a)$$

s.t $\boldsymbol{\mu}, \boldsymbol{\vartheta} \geq 0$ (16b)

The adapted dual problem in (16) is a convex function of dual variables ($\boldsymbol{\mu}, \boldsymbol{\vartheta}$) since the second partial derivatives with respect to dual variables $\boldsymbol{\mu}$ and $\boldsymbol{\vartheta}$ exist with a non-negative value [21]. Based on above analysis, the centralized subgradient solution for the dual problem in (10) is given by Algorithm 1.

2.3.1 Centralized Subgradient Algorithm (Algorithm 1)

The following algorithm gives the solution of dual variables $\boldsymbol{\mu}$, $\boldsymbol{\vartheta}$ and calculates the maximum throughput values given in problem (16).

Step 1: Establish some positive initial values for dual variable vectors $\boldsymbol{\mu}$ and $\boldsymbol{\vartheta}$ and fix a sufficient number of iterations i_{max} and step size $t^i = \frac{a}{b+i}$ where a > 0, b≥ 0.

Step 2: Initialize the association of all users with a serving MBS / FBS. Each $k\epsilon K$ decides its serving BS $j\epsilon J$ on current dual variables $\boldsymbol{\mu^i}$ and $\boldsymbol{\vartheta^i}$ according to $j_k^i = \underset{j}{\operatorname{argmax}} \frac{c_{k,j}}{\mu_j+\vartheta_k}$.

Step 3: Calculate the number of users attached to the BS *j* for the *i*-th iteration and let it be K_j^i.

Step 4: Update the dual variables μ_j^{i+1} and ϑ_k^{i+1} according to the current values of dual variables for the *i*-th iteration (μ_j^i and ϑ_k^i) by taking the partial derivatives of (16) with respect to μ_j and ϑ_k respectively according to:

$$\mu_j^{i+1} = \max\left(\left(\mu_j^i + t^i\left(\sum_{k\epsilon K_j^i}\left(\mu_j + \vartheta_k\right)^{-1} - S_j\right)\right), 0\right) \text{ and}$$

$$\vartheta_k^{i+1} = \max\left(\left(\vartheta_k^i + t^i\left(\left(\left(\mu_j + \vartheta_k\right)^{-1} - 1\right)\right)\right), 0\right).$$

Step 5: Go to step 2 and continue while $i < i_{max}$.

Algorithm 1 presents a globally optimal solution for the convex dual problem (16) where during each iteration, the dual variables (Step 4) provide association based on the maximum throughput for each user (Step 2). However, the results observed may not be optimally feasible but nearby feasible for the primal problem (6) because of the distinct characteristic of the primal problem and limited number of iterations. The dual variables obtained by subgradient algorithm are nevertheless known to provide a near optimal solution for the primal problem [30].

2.4 User-Cell Association Methods

In conventional cellular networks operating at HF, the user-cell association decision is usually performed by maximum RSRP. In this case, the user is associated with the BS which offers the highest received power to it where the received power is a function of channel gain which includes pathloss and shadowing (large-scale). The effect of shadowing varies slowly in conventional networks. However, this variation in shadowing is slower in mmWave cellular networks than conventional networks due to blockages on the received power. Therefore, in mmWave cellular networks, the slowly varying fluctuations caused by shadowing may not be accounted for user-cell association. Because of this reason, cell association performed according to smallest pathloss where each user associated with a BS which provides the smallest pathloss to it [31]. Here, Section 2.4 gives the definition of smallest pathloss and maximum downlink capacity cell association schemes in which the load of a BS is not taken into account, and a game theoretical user-centric association scheme.

2.4.1 Smallest Pathloss User-Cell Association Model

This method associates a user with a BS which provides the smallest pathloss. After the association decision is made by every user, the activity fraction of a user and its serving BS is calculated by (6). This method provides a unique association for all users. In this case, user k will have a value of $\alpha_{k,j}$ to only BS j. Corresponding equation is given in (17).

$$\alpha_{k,j} = \begin{cases} \frac{S_j}{|K_j|}, & \text{for } j = j_k \\ 0, & \text{for } j \neq j_k \end{cases} \quad (17).$$

2.4.2 Maximum Downlink Capacity User-Cell Association Model

In the system model used in this thesis, macro BSs have less bandwidth than femto BSs which operate at mmWave frequency. The very high bandwidth enhances the capacity in mmWave spectrum. In [11], the association is made according to maximum instantaneous rate (bps/Hz). Even if bandwidth is taken into account for association in [11], the association is not going to change, since both macro BSs and femto BSs operate at HF sharing same bandwidth. However, in mmWave massive MIMO system, instead of maximum instantaneous rate (bps/Hz), using maximum downlink capacity (bps) is more appropriate than maximum instantaneous rate. A user k chooses a BS j which provides the maximum downlink data rate. After that, it calculates its activity fraction to the serving BS by (6).

2.4.3 A Game Theoretical Distributed Approach for User-Cell Association

In this section, an algorithm is adapted from [11] to find the optimal association of users to BSs. The algorithm requires load information of the BSs during the association decision process as opposed to the conventional user-cell association performed by maximum downlink capacity, maximum RSRP or smallest pathloss schemes. The presented user-centric distributed algorithm performs the association based on the maximum throughput, i.e. each user aims to associate with a BS which maximizes its throughput in a selfish manner. Compared to the centralized subgradient, this distributed non-cooperative game theoretical approach provides a low complexity implementation yet near optimal solution to (10).

Consider a pertinent scenario where each BS in the network allocates its transmission resources to its associated users in a fair way (PF). However, each BS is assumed to be associated with at least S_j users (indicating fully loaded BSs) in the network. On the other hand, each user can only be served by only one BS (unique association). For load-based distribution implementation, a typical mmWave massive MIMO system with heavily loaded BSs (MBSs, FBSs) is considered.

In the distributed approach, a user tends to change its association configuration until there is no more BS which offers better throughput. At this saturation point, all the users in the network reach an equilibrium point referred as "Nash equilibrium". When the scheduler operates in PF mode, every user uniquely reaches the Nash equilibrium if the distributed algorithm is performed selfishly [32]. The condition for the discussed Nash equilibrium using PF is given by

$$\frac{S_j c_{k,j}}{|K_j|} \geq \frac{S_l c_{k,l}}{|K_l|+1}, \forall\, k \epsilon K, \forall\, j, l \epsilon J, l \neq j \tag{18}$$

2.4.4 User-Centric Distributed Algorithm (Algorithm 2)

<u>Step 1</u>: Initialize the iteration count and the number of migrations observed by all users as i = 0 and m = 0 respectively. Fix a sufficient number of iterations i_{max} and a realistic switching probability p.

Step 2: Every user $k \epsilon K$ updates it BS-association during each iteration and switches from its current serving BS k to a different BS l when the following conditions are met:

$$\frac{s_l c_{k,l}}{|K_l|+1} > \frac{s_j c_{k,j}}{|K_j|} \geq, \forall\, k \epsilon K, \forall\, j, l \epsilon J, l \neq j$$ and

$$rand < \, p^{(m_{i_k}+1)}.$$

Step 3: During each iteration i, increment the migration count $m_{i_k}$by 1 for each user k whenever k migrates from its current BS j to a different BS l (i.e. when conditions from Step 2 are satisfied).

Step 4: Go to Step 2 and continue while $i < i_{max}$.

Chapter 3: Development of System Level Simulator

Although there exist a number of freely available network simulators such as NS-3, Vienna LTE simulator, LTE-sim, etc., they are complex and not easy to modify. As a result, the dependency between simulator modules makes implementation of new algorithms or modifications like mmWave pathloss model a time-consuming process. Additionally, most available simulators are concerned with physical layer properties like bit error rate (BER) whereas this thesis's interest rests in system level performance analysis and evaluation. To overcome these issues, a system level simulator was designed as a part of this study which incorporated mmWave pathloss model, massive MIMO systems and ultra-dense HetNets.

As a starting point, an existing MATLAB based system level LTE simulator which was developed by Wireless Systems Research Lab, Hitachi America Ltd. has been chosen. The simplicity of this system level LTE simulator enables easy modification and implementation of additional functions and network topologies. The detail of the simulator is described in this chapter.

The organization of Chapter 3 is given as follows. In Section 3.1, the specifications of the existing MATLAB based Hitachi system level simulator called *Cellular Network Topology Toolbox* is given. In section 3.2, the shortcomings of the simulator are addressed. Finally, in Section 3.3, the modifications and improvements made in the simulator are introduced.

2.1 Cellular Network Topology Toolbox

This simulator has been developed under MATLAB 8.2.0.701(R2013b) to support both macro and small cell network topologies by considering the 3GPP specifications. It can be run under MATLAB 8.2.0.701(*R*2013*b*) or higher versions.

3.1.1 The Network Scenarios supported in the Simulator

The simulator is able to perform simulation for only four different urban scenarios. All the parameters used for each scenario are taken from [31]. These scenarios are explained below:

1. **Urban Macro**: Uniformly distributed users are served only by macro BSs which are located at the center of each hexagonal area. Each macro BS has very large cell area and serves only outdoor users.
2. **Urban Micro**: Micro BSs have smaller cell radius and serve both indoor and outdoor users uniformly distributed in a dense urban environment.
3. **HetNet Conf 1**: Macro BSs are located at the center of each cell and small cells and users are uniformly located around macro BSs. In this scenario, both macro and small BSs serve both indoor and outdoor users.
4. **HetNet Conf 4b**: This model presents a hot-spot scenario where macro BSs are located at the center of each cell and small cells are uniformly distributed around macro BSs and a fraction of users are located around small cells with uniform density. In this scenario, both macro and small BSs serve both indoor and outdoor users.

3.1.2 Channel Model

The simulator supports only single antenna BSs and users. It calculates channel gain as a function of pathloss, shadowing antenna gain and feeder loss. The feeder loss is taken into account only for urban macro scenario and it is given by

$$P_{RX} - P_{TX} = P_L + SF + AG + L_{misc} \quad (19)$$

where P_{RX}, P_{TX}, P_L, SF, AG, L_{misc} are the receive power, transmit power, distance dependent pathloss, shadowing, antenna gain and feeder loss respectively. Pathloss and shadowing takes different values based on frequency and whether a user is indoor or outdoor and whether a link is NLOS or LOS.

The simulator supports 7 cells or 19 cells with 3 sectors. The 7 cells with 3 sector hexagonal network layout is given in Figure 3.

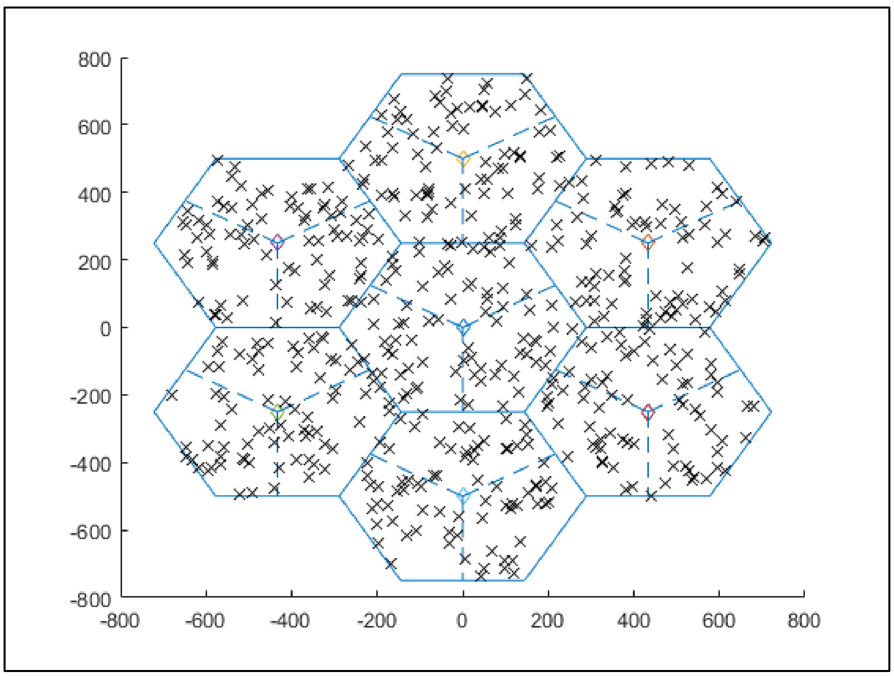

Figure 3 The hexagonal network layout

3.1.3 Main Modules of the Simulator

The description of the main modules in the existing simulator are given in Table 2.

Table 2 Main modules of the Simulator

Module Name	**Description**
GenMacroTopology	Generates the position of eNBs in hexagonal network layout.
GenRRH	Generates the position of small cells per cell with uniform distribution by considering the distance constraints.
GenUEPosForMacro	For urban macro and urban micro scenarios, the function generates uniformly distributed user position in each cell with distance constraints.
GenUEPosForHetNet1	For HetNet1 scenarios, the function generates uniformly distributed user position in each cell with distance constraints.
GenUEPosForHetNet4b	For HetNet4b scenarios, the function generates uniformly distributed user position in each cell with distance constraints. However, a fraction of users are located around small cells.
GenChannelIUMa	Generates large scale channel between outdoor users and BSs for urban macro scenario.
GenChannelIUMi	Generates large scale channel between outdoor and indoor users and BSs for urban micro scenario.
GenChannelHetNet	Generates large scale channel between outdoor and indoor users and BSs for urban HetNet scenarios.
CalcAntennaGain	Generates the 3D antenna gain considering both horizontal and vertical antenna lobes for a user to all BSs.
UE2BSAssoc	Associates a user with a BS based on maximum RSRP within the handover margin selected.
PlotNetworkTopology	Plots the hexagonal network layout.

2.3 Shortcomings of the Cellular Network Topology Toolbox

The simulator explained above is a basic system level LTE simulator. Although it is very simple to modify, it needs to be improved due to its shortcomings with respect to the system model presented previously. The first shortcoming of the simulator is that it does not consider inter-cell interference and pilot contamination. It should be added into simulator because of the fact that technologies like massive MIMO, require accurate channel estimation in TDD mode. However, the use of non-orthogonal pilot signals used for channel estimation causes pilot contamination. The second limitation of the simulator is that it allows us to perform a simulation with only one antenna at transmitter and receiver. Therefore, a module should be added to simulate MIMO or massive MIMO systems. Operating a network in only HF spectrum should not be the only option and mmWave pathloss model should be considered in the simulator. Additionally, beamforming is a technique which can increase the SINR value but there is no beamforming technique implemented in the simulator. Another shortcoming is that slow fading is not modeled in the simulator. Finally, the load balancing is a significant way to increase the user throughput particularly when the heterogeneity is considered. Offloading the macro BSs with some user-cell association techniques should be implemented into the simulator.

2.4 What is new in the improved simulator?

Based on the shortcomings explained in Section 3.2, some new functions which can cope with the shortcomings of the simulator are implemented. In addition to that, two new network scenarios which do not concern with sectoring into the simulator are added. The descriptions of functions to create these topologies are given below:

1. **HetNet Conf Rec**: Macro BSs are located at the center of square areas. Small cells are uniformly distributed within the rectangular area and a fraction of users are located uniformly around macro BSs with higher density.

2. **HetNet Conf 2**: Macro BSs are placed in the center of each cell and each cell has three hot-zones with higher user density and each hot-zone has randomly placed 4 small cells in it. Users are generated with uniform distribution.

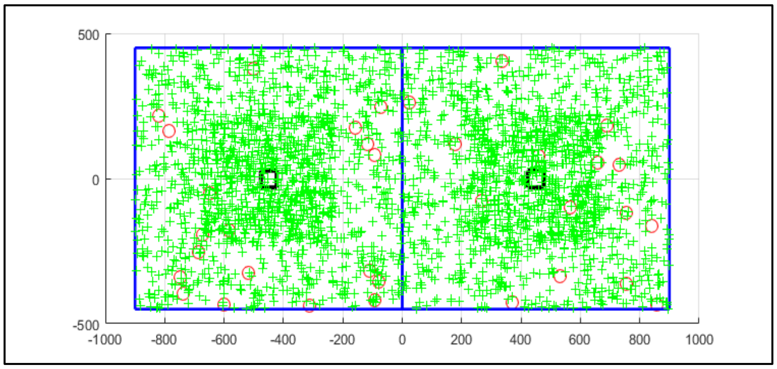

Figure 4 The rectangular network layout

Figure 4 and 5 shows the network layout for HetNet Conf Rec and HetNet Conf 2 respectively.

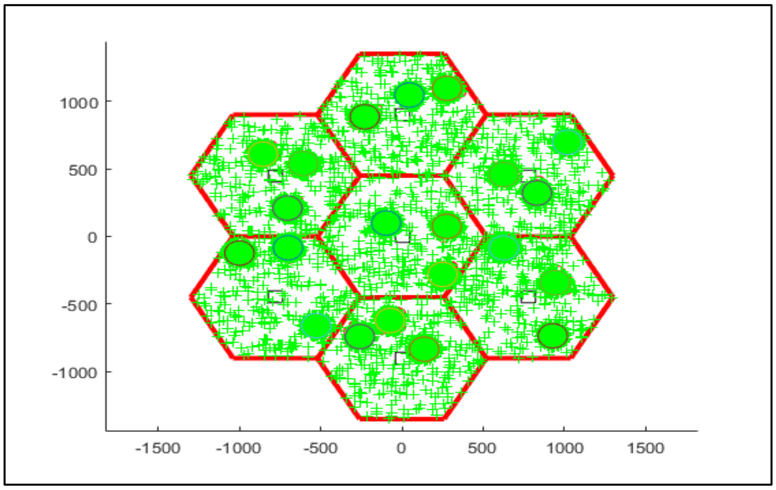

Figure 5 The hexagonal network layout for HetNet Conf 2

The following Table 3 introduces the description of new modules related to HetNet Conf 2 implemented in the simulator.

Table 3 Modules related to HetNet Conf 2

Module Name	**Description**
CalcSINR	Calculates the SINR value in downlink with zero forcing beamforming, conjugate beamforming and analog beamforming by considering the inter-cell interference.
GenHotSpotCenter	Generates randomly placed hot-zones within each cell.
GenPilotSignal	Generates mutually orthogonal pilots. It allocates a set of mutually orthogonal pilots to be shared amongst the macro BSs whereas the small BSs share a different set of mutually orthogonal pilots shared amongst small BSs.
GeneratesUEPosForHetNet2	Generates uniformly distributed user position with higher density within hot-zones.
CalcThrDistributed	Associates a user with a BS based on a game theoretical user-centric distributed method by considering the load of BSs. Users selfishly try to maximize their throughput by running the algorithm given in Section 2.4.4.
CalcThrSubgradient	It presents a solution for a convex problem which aims to find optimal user-cell association by running the algorithm given in Section 2.3.1
CalcThrMaxRate	Associates a user with a BS which offers maximum downlink rate. It does not consider the load of BSs.
CalcThrSmallestPL	Associates a user with a BS which offers the smallest pathloss. It does not consider the load of BSs.
GenChannelForMasMIMO	Generates M_j x S_j channel matrix where M_j and S_j are the number of antennas and number of downlink data stream and calculates PL, SF and slow fading modeled as Rayleigh for massive MIMO and mmWave massive MIMO.
GenRRHwithinHotZone	Generates small cells randomly placed within each hot-zone.

Table 4 presents the definition of some modules related to HetNet Conf Rec. Additionally, all the user-cell association schemes and some functions like CalcSINR, GenPilotSignal and GenChannelForMasMIMO given in Table 4 can be used for HetNet Conf Rec as well.

Table 4 Modules related to HetNet Conf Rec

Module Name	**Description**
GenMacroTopForRec	Generates location of eNBs for rectangular area. It positions them in the center of two square areas showed in Figure 4.
GenRRHForRec	Generates small BSs within rectangular area, uniformly distributed, by considering distance constraints.
GenUEPosForRec	Generates UE position with a non-homogeneous Poisson point process with higher density around macro BSs by considering distance constraints.
PlotRecNetworkTop	Plots the rectangular network layout.

Chapter 4: Experimental Evaluation

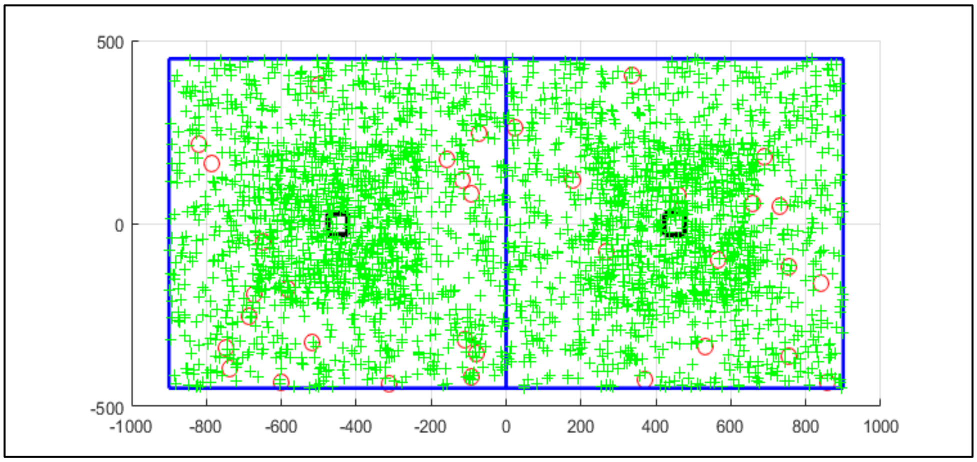

Figure 6 Network Layout

This chapter evaluates the performance of user-cell association algorithms for massive MIMO deployment in two-tier network under two different set ups:

1. HF-HF (both tiers operating at HF).

2. HF-mmWave (macro BSs operating at HF while femto BSs at mmWave frequency).

The baseline algorithms used for comparison with the centralized subgradient algorithm and distributed user-centric algorithm both adapted from [11] are the maximum downlink data rate and smallest pathloss schemes.

This experiment considers a downlink two-tier UDHN consisting of two macro BSs having 100 antennas each with 46 dBm transmit power and randomly deployed 34 femto BSs having 40 antennas each with 35 dBm transmit power in a rectangular region of dimensions 900m x 1800m. The macro BSs are placed in the center of two square areas identifying hot-zones (higher user concentration) for the non-uniform user distribution in the simulation area. Each hot-zone contains about 1/3rd of the total user-count with the

Table 5 Simulation Parameters

Parameter	Value
Bandwidth of mmWave femto BS, Carrier Frequency	800 MHz, 38 GHz
Bandwidth of macro BS, Carrier Frequency	20 MHz 2 GHz
Rectangular Area	900m x 1800m
Number of users	3000
Q, T	3, 7
N_F, T_K, k_b	7dB, 290^{o} Kelvin, 1.38 x 10^{-23} J/Kelvin
Two-slope LOS pathloss model of HF macro BS	22log(d) + 34.02 + X_σ, if 10m < d <320m 40log(d) – 11.02 + X_σ, if 320m < d<5000m $\sigma = 4$
NLOS pathloss model of HF macro BS	39.1log(d) + 19.56 + X_σ, $\sigma = 6$
Two-slope LOS pathloss model of HF femto BS	22*log(d) + 34.02+ X_σ, if 10m < d <120m 40log(d) – 3.36 + X_σ, if 120m < d<5000m $\sigma = 3$
NLOS pathloss model of HF femto BS	36.7log10(d) + 30.53 + X_σ, $\sigma = 4$
Pathloss model of mmWave femto BS	20log($\frac{4\pi}{\lambda}$) + 10$\alpha_{LOS(or\ NLOS)}$log(d) + X_σ LOS: $\sigma = 4.6$, α_{LOS}= 1.9 NLOS: $\sigma = 12.3$, α_{NLOS}= 3.3
Probability of LOS (pLOS) for mmWave femto BS	min(18/d, 1)(1 - $e^{-\frac{d}{36}}$) + $e^{-\frac{d}{36}}$
Probability of LOS (pLOS) for HF macro BS	min(18/d, 1)(1 - $e^{-\frac{d}{63}}$) + $e^{-\frac{d}{63}}$
Transmit power of macro BS and femto BS respectively	46 dBm, 35 dBm
A_j for macro BS and femto BS respectively	100, 40
S_j for macro BS and femto BS respectively	10, 4
User height	1.5m
Base station height	Femto BS: 10m, Macro BS: 25m
Radius of femto BS	40m
p	0.1

spatial distribution varying in each simulation run to provide more accurate results. The femto BS deployment is uniform throughout the simulation area as shown in the network snapshot in Figure 6. The macro BSs, femto BSs and users are represented by □, ○ and + respectively.

An intra-BS interference free network is assumed by allocating a set of 10 orthogonal pilots to be shared amongst the macro BSs whereas the femto BSs share a different set of 4 orthogonal pilots for channel estimation. A detailed list of simulation parameters is presented as Table 5.

The pathloss model for mmWave small cells is taken from [4] and a two-slope pathloss models for macro cells and small cells both operating at HF spectrum are assumed [31].

Figure 7 presents the performance comparison of the user-cell association algorithms explained in Chapter 2 in terms of 5-percentile user throughput for the mmWave massive MIMO network layout given in Figure 6.

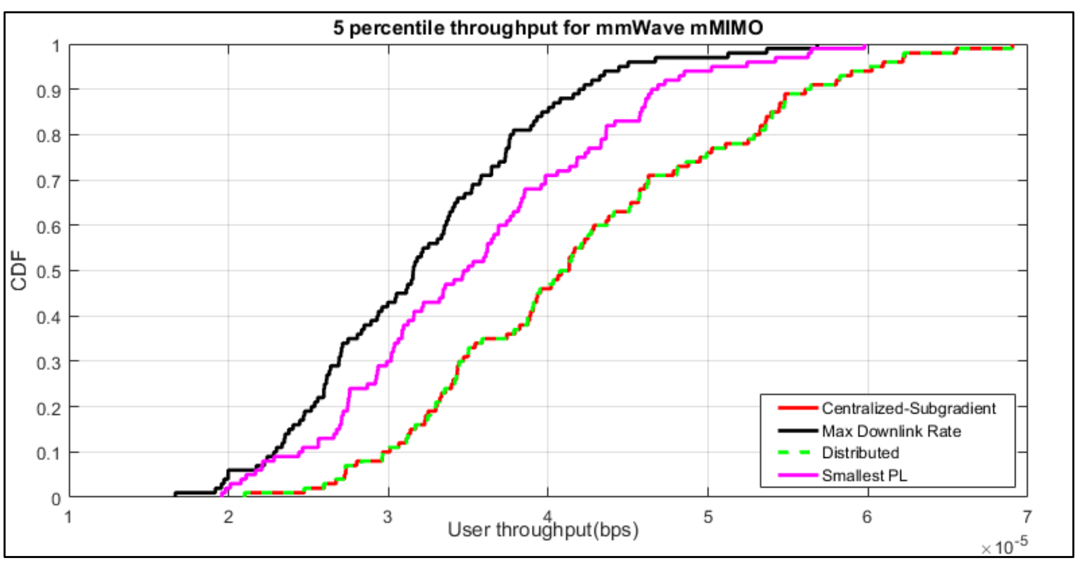

Figure 7 Performance comparison of algorithms in terms of 5-percentile throughput in mmWave band

The 5-percentile user throughputs result in Figure 7 shows that the adapted centralized subgradient and game theoretical user-centric distributed algorithms outperform the baseline schemes. Maximum downlink data rate method demonstrates the worst performance in terms of the user throughput while the modified algorithms from [11] show almost identical results. However, maximum downlink data rate method demonstrates better performance than the smallest pathloss method for HF-HF massive MIMO system whose 5-percentile user throughput is given in Figure 8. The results indicate that for a massive MIMO system operating at HF, the adapted algorithms provide better performance but the worst performance is observed by smallest pathloss.

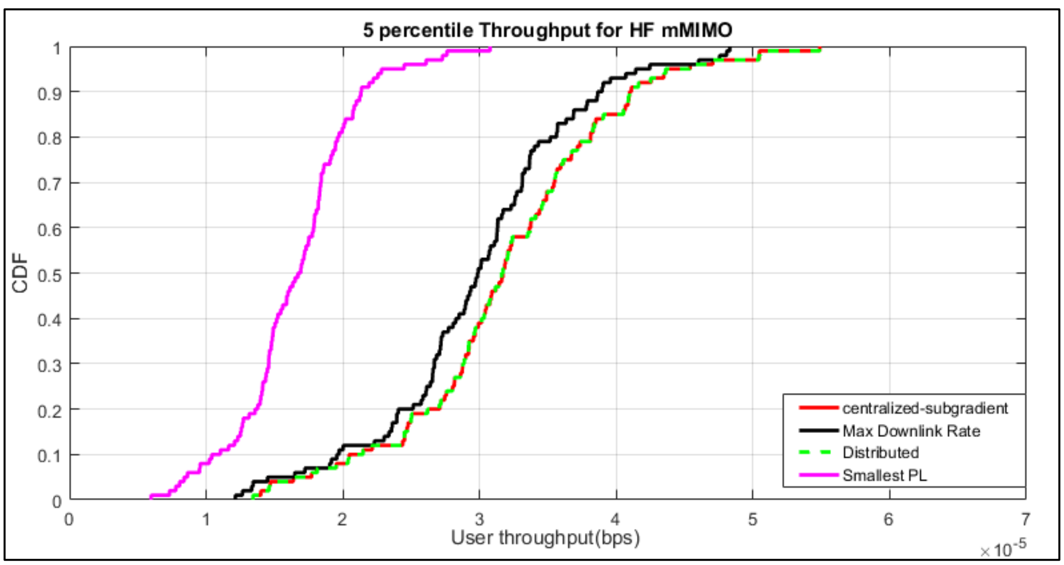

Figure 8 Performance comparison of algorithms in terms of 5-percentile throughput in HF band

Figure 9a and 9b reveal the indistinguishable performance of the centralized subgradient with the user-centric distributed algorithm. In addition to that, in case of arithmetic mean throughput, the performance of the smallest pathloss method is almost indistinguishable from the performance of centralized subgradient and game theoretical user-centric distributed algorithms.

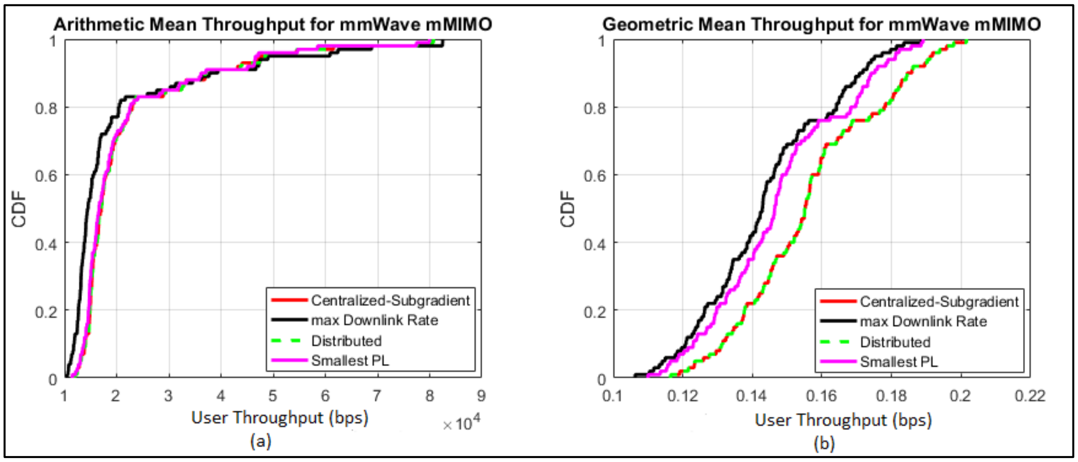

Figure 9 Arithmetic and geometric mean throughputs in mmWave massive MIMO

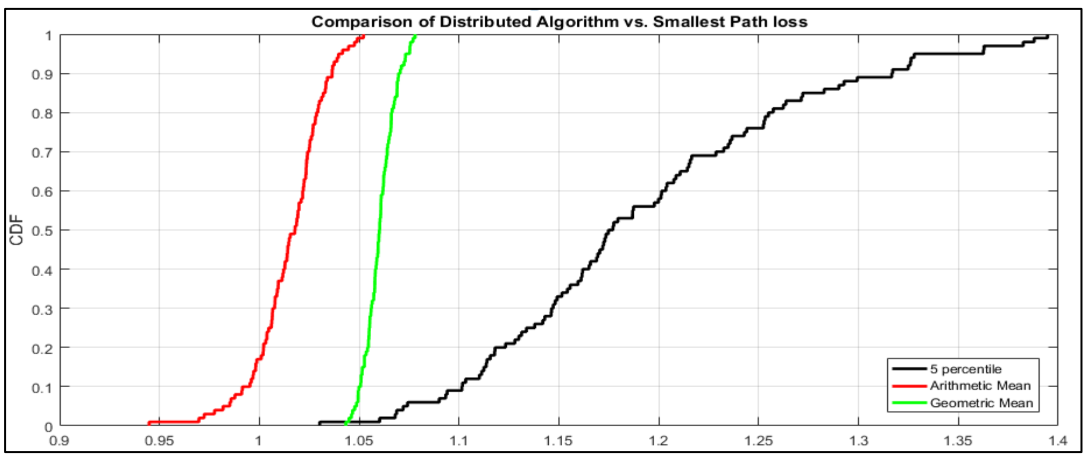

Figure 10 Comparison of distributed algorithm with smallest pathloss algorithm

In Figure 10, the performance of the distributed and smallest pathloss user association algorithms is compared by taking the ratio of their respective throughput statistics and plotting the CDF of the results obtained in each iteration. Gains are observed for each of the data rate statistics presented in Figures 7, 9a and 9b. For instance, it is seen that for about 60% of the iterations, a gain of 20% is achieved in the 5-percentile data throughput.

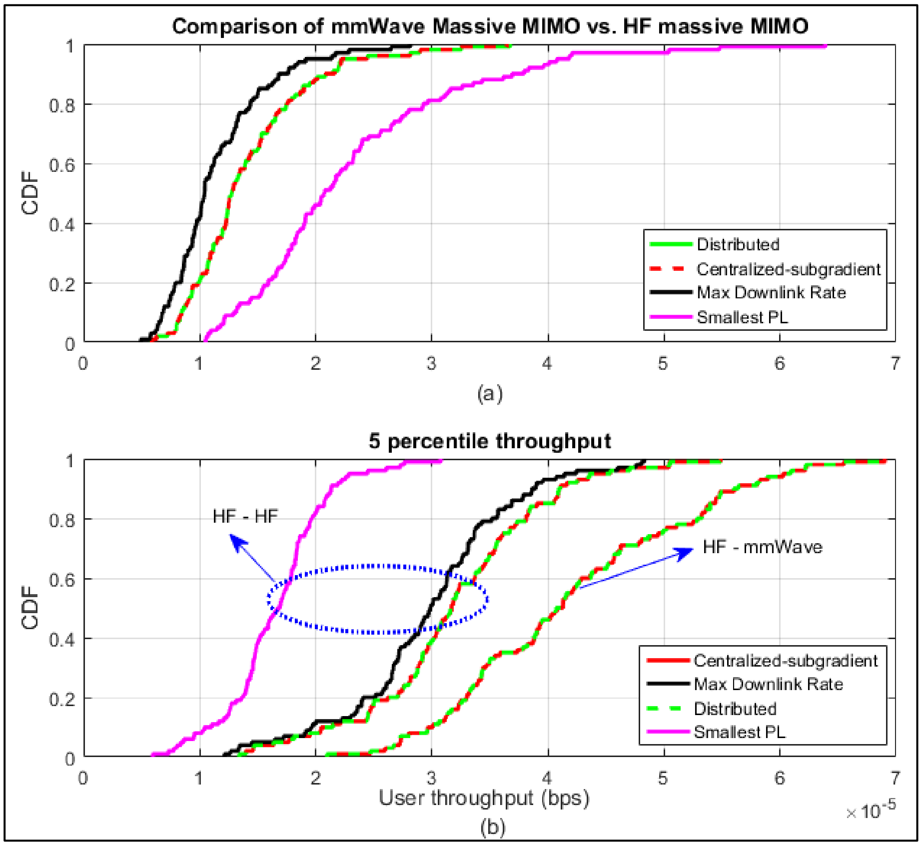

Figure 11 Comparison HF-HF versus HF-mmWave network

Figure 11a presents a comparison of the 5-percentile data throughput performance gain when the femto BS-tier is operated at mmWave spectrum instead of the HF band. The ratio of the 5 percentile statistics is obtained for each association scheme in mmWave vs HF massive MIMO schemes and the CDF results are plotted for analysis. The results indicate that with smallest pathloss association, about 50% users will experience 2x data rates increase when femto BS-tier is operated in the mmWave spectrum. The results are intuitive since the drastic variations in mmWave channel allow this association scheme to be better suited at mmWave as compared to the HF spectrum. The increase in the data rates with centralized subgradient and distributed user-centric in mmWave spectrum is marginal as given in Figure 11a. To analyze the overall data rate improvement in the mmWave spectrum, the 5-percentile throughput of the optimal association schemes in Figure 11b is compared and 30% increase is observed for almost half of the realizations.

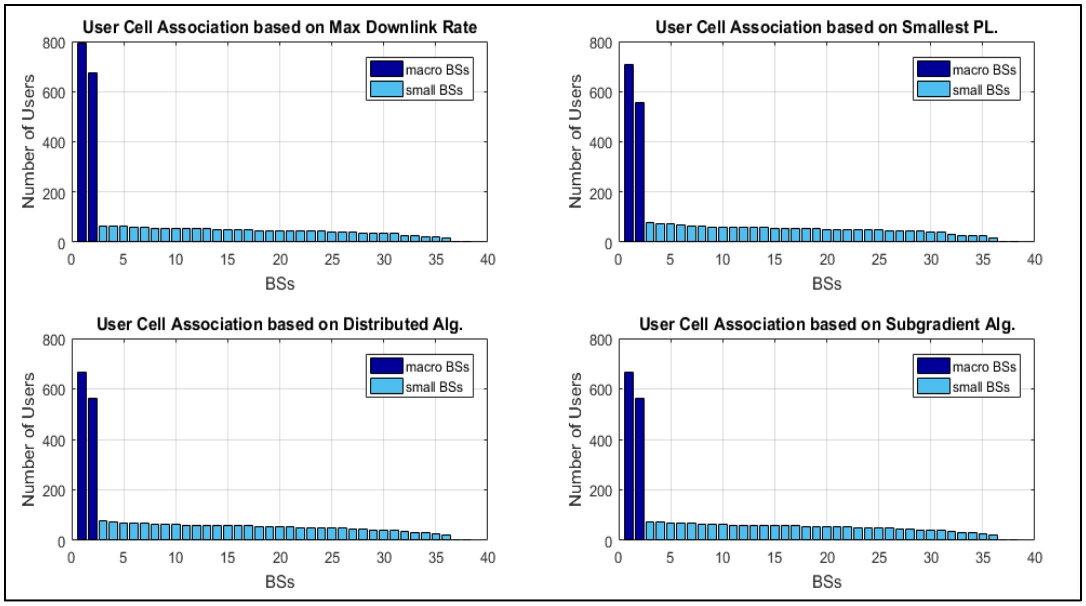

Figure 12 Load distribution for user-cell association algorithms for mmWave network

Figure 12 presents the load association of users with the macro BSs and femto BSs under the four different user-cell association schemes analyzed in this thesis. The number of users associated with each BS in descending order is plotted while clearly demarcating the macro BS and femto BS tier association. In terms of offloading the macro BSs, the game theoretical distributed user-centric and centralized subgradient algorithms, which are dependent upon the load of BSs, outperform the baseline algorithms. The maximum downlink rate association shows worst performance with high loads on the macro BSs. The balanced distribution of the load within BSs of each tier shows efficient load balancing capabilities of the proposed algorithm.

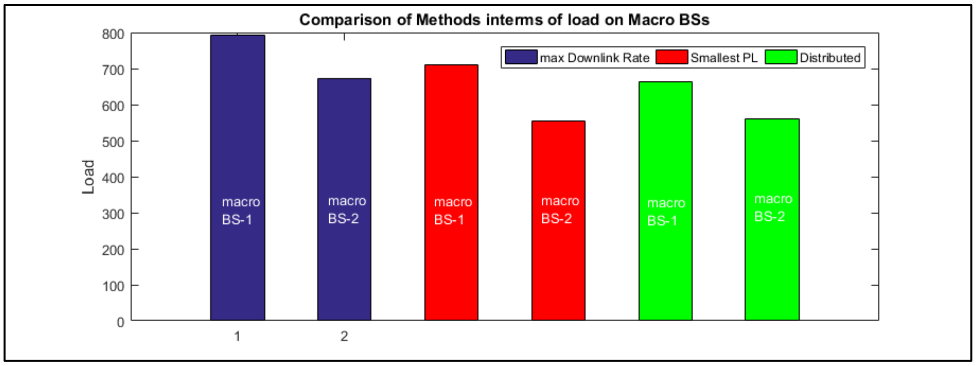

Figure 13 Load distribution of macro BSs

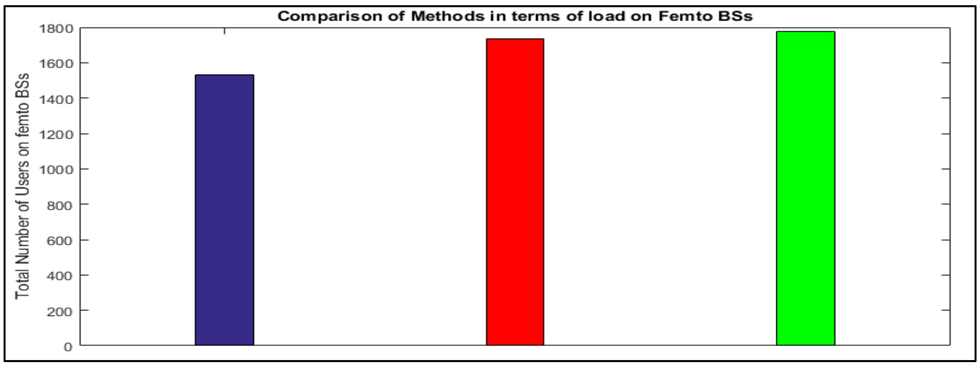

Figure 14 Load distribution of femto BSs

Figure 14 shows the number of users attached to the each macro BS when the simulation is run according to algorithms given in the Figure 13 legend. The worst performance is observed by maximum downlink data rate. However, in the distributed algorithm, macro BSs have less number of users as compared to the other algorithms with highest 5- percentile throughput.

Figure 15 shows the total number of users associated with femto BSs in the network and it can be deduced that the distributed algorithm provides more relaxation on the macro BSs in terms of the load.

Chapter 5: Conclusion and Future Work

The primary objectives of this thesis were to find out which user-cell association method will work best for next generation mmWave massive MIMO networks, and development of a MATLAB based system level simulator for HetNets.

To accomplish the desired goals, four different user-cell association methods have been implemented after a detailed literature review of relevant studies on user-cell association. Then, a comparative analysis of the algorithms studied was presented for a multi-tier (UDHNs) with massive MIMO deployment in both HF and mmWave spectrum. Additionally, a simple MATLAB based system level LTE simulator was modified and improved for this work. The comparative analysis of the algorithms was performed by using a simulator developed in this thesis for mmWave massive MIMO UDHNs.

The four user-cell association methods analyzed in this thesis were implemented in the simulator. The first method is called the centralized subgradient algorithm which aims to maximize the overall proportionally fair network utility function by maximizing user throughput. The basic idea of the algorithm is inspired from [11] and the optimization problem is adapted with an additional difference. The difference is the identification of a new utility function which is a function of bandwidth in order to analyze the effect of large bandwidth available in mmWave spectrum for user-cell association and user throughput. The second method is also adapted from [11] but again bandwidth is considered as a part of the utility function. The third and fourth methods are called maximum downlink rate and smallest pathloss respectively. The effect of each user-cell association method was investigated using different key performance indicators including the user throughput and cell load. The performance of both mmWave massive MIMO and HF massive MIMO networks are observed by implementing the aforementioned algorithms. Results indicate that both centralized subgradient and game theoretical user-centric distributed algorithms outperform rest of the algorithms and yield higher throughput in mmWave network deployment as compared to the HF network deployment. However, it is observed that smallest pathloss model is more suited for mmWave deployment then HF deployment. It is because the shadowing varies slowly in conventional networks, however; it is almost negligible in mmWave communication systems because of the blockages in the received power [31]. The simulator results presented in this thesis prove this statement. While the performance of game theoretic user-centric distributed association method almost matches the performance of centralized subgradient association method, the simplicity in its implementation without requiring a centralized unit renders it as a suitable candidate for user-cell association in future mmWave massive MIMO.

To sum up, the mmWave spectrum can be one of the best candidates to boost user throughput along with massive MIMO technology, since it enables packing of large antenna arrays in a smaller area. The increment in the number of antennas can provide more antenna gain with proper beamforming techniques to overcome the very large pathloss of mmWave signals. Additionally, the large amount of mmWave bandwidth can bring an enhancement of the user throughput in conjunction with the gains obtained through large antenna arrays.

While the objectives of this thesis have been achieved, the user-cell association algorithm requires further refinements including cell load considerations. Although the adapted algorithms from [11] consider the load of base stations, these algorithms do not have any threshold for the number of users for both macro and femto BSs. A new association scheme which can limit the number of users which will attach to a BS with a certain threshold can be investigated as a part of the future study. In addition to that, further improvements can be proposed by incorporating cell individual offset (CIO) to artificially increase the coverage area of small cells. Moreover, SINR biasing can be considered to improve the algorithms as well. Furthermore, although a system level simulator has been developed as a part of this thesis which can cope with the shortcomings given in Section 3.2 by modifying an existing simulator, it can be further improved in the future by adding user mobility, handover procedures and uplink scheduling.

References

[1] CISCO, “Cisco visual networking index: Mobile data traffic forecast update, 2013 to 2018,” San Jose, CA, USA, 2014.

[2] J. G. Andrews, S. Buzzi, W. Choi, S. V. Hanly, A. Lozano, A. C. K. Soong, and J. C. Zhang, "What Will 5G Be?," in ***IEEE Journal on Selected Areas in Communications***, vol. 32, no. 6, pp. 1065-1082, June 2014.

[3] Z. Pi and F. Khan, "An introduction to millimeter-wave mobile broadband systems," in ***IEEE Communications Magazine***, vol. 49, no. 6, pp. 101-107, June 2011.

[4] T. S. Rappaport, G. R. MacCartney, M. K. Samimi and S. Sun, "Wideband Millimeter-Wave Propagation Measurements and Channel Models for Future Wireless Communication System Design," in ***IEEE Transactions on Communications***, vol. 63, no. 9, pp. 3029-3056, Sept. 2015.

[5] F. Rusek ***et al***., "Scaling Up MIMO: Opportunities and Challenges with Very Large Arrays," in ***IEEE Signal Processing Magazine***, vol. 30, no. 1, pp. 40-60, Jan. 2013.

[6] T. L. Marzetta, "Noncooperative Cellular Wireless with Unlimited Numbers of Base Station Antennas," in ***IEEE Transactions on Wireless Communications***, vol. 9, no. 11, pp. 3590-3600, November 2010.

[7] Mobile, China. "C-RAN: the road towards green RAN." *White Paper, ver* 2 (2011). http://labs.chinamobile.com/cran/wpcontent/uploads/CRAN_white_paper_v2_5_EN.pdf

[8] J. G. Andrews, S. Singh, Q. Ye, X. Lin and H. S. Dhillon, "An overview of load balancing in hetnets: old myths and open problems," in ***IEEE Wireless Communications***, vol. 21, no. 2, pp. 18-25, April 2014.

[9] Rappaport, Theodore S., et al. *Millimeter wave wireless communications*. Pearson Education, 2014.

[10] 3rd Generation Partnership Project (3GPP), “3GPP TR#36.872,” 2013.

[11] D. Bethanabhotla, O. Y. Bursalioglu, H. C. Papadopoulos and G. Caire, "Optimal User-Cell Association for Massive MIMO Wireless Networks," in ***IEEE Transactions on Wireless Communications***, vol. 15, no. 3, pp. 1835-1850, March 2016.

[12] D. Bethanabhotla, O. Y. Bursalioglu, H. C. Papadopoulos and G. Caire, "User association and load balancing for cellular massive MIMO," ***2014 Information Theory and Applications Workshop (ITA)***, San Diego, CA, 2014, pp. 1-10.

[13] 3GPP, "Technical specification group radio access network; Small cell enhancements for E-UTRA and E-UTRAN," TR 36.872, V12.1.0, Dec. 2013.

[14] A. Ghosh et al., "Heterogeneous cellular networks: From theory to practice," IEEE Commun. Mag., vol. 50, no. 6, pp. 54–64, Jun. 2012.

[15] ˙I. Güvenç, M.-R. Jeong, ˙I. Demirdo˘gen, B. Kecicio˘glu, and F. Watanabe, "Range expansion and inter-cell interference coordination (ICIC) for picocell networks," in Proc. IEEE VTC Fall, Sep. 2011, pp. 1–6.

[16] J.-W. Lee, R. R. Mazumdar, and N. B. Shroff, "Joint resource allocation and base-station assignment for the downlink in CDMA networks," IEEE/ACM Trans. Netw., vol. 14, no. 1, pp. 1–14, Jan. 2006.

[17] K. Son, S. Chong, and G. de Veciana, "Dynamic association for load balancing and interference avoidance in multi-cell networks," IEEE Trans. Wireless Commun., vol. 8, no. 7, pp. 3566–3576, Jul. 2009.

[18] L. Jiang, S. Parekh, and J. Walrand, "Base station association game in multi-cell wireless networks," in Proc. IEEE WCNC, 2008, pp. 1616–1621.

[19] Q. Ye, O. Y. Bursalioglu, H. C. Papadopoulos, C. Caramanis and J. G. Andrews, "User Association and Interference Management in Massive MIMO HetNets," in ***IEEE Transactions on Communications***, vol. 64, no. 5, pp. 2049-2065, May 2016.

[20] G. Athanasiou, P. Weeraddana, C. Fischione, and L. Tassiulas, "Optimizing client association for load balancing and fairness in millimeter-wave wireless networks," IEEE/ACM Trans. Netw., vol. 23, no. 3, pp. 836–850, 2015.

[21] B. Xu, Y. Chen, M. Elkashlan, T. Zhang and K. K. Wong, "User association in massive MIMO and mmWave enabled HetNets powered by renewable energy," ***2016 IEEE Wireless Communications and Networking Conference***, Doha, 2016, pp. 1-6.

[22] Molisch, Andreas F. *Wireless communications*. Vol. 34. John Wiley & Sons, 2012.

[23] B. M. Hochwald, T. L. Marzetta and V. Tarokh, "Multiple-antenna channel hardening and its implications for rate feedback and scheduling," in ***IEEE Transactions on Information Theory***, vol. 50, no. 9, pp. 1893-1909, Sept. 2004.

[24] K. Son, S. Chong, and G. de Veciana, "Dynamic association for load balancing and interference avoidance in multi-cell networks," IEEE Trans. Wireless Commun., vol. 8, no. 7, pp. 3566–3576, Jul. 2009.

[25] "Technical Specification Group Radio Access Network; Study on 3D Channel Model for LTE (Release 12), document 3GPP TR 36.873," 3GPP, Sep. 2014.

[26] 3GPP TR 36.814, “Further advancements for E-UTRA physical layer aspects (Release 9),” http://www.3gpp.org/ftp/Specs/archive/36series/36.814/36814-900.zip , Mar. 2010.

[27] T. L. Marzetta, "Noncooperative Cellular Wireless with Unlimited Numbers of Base Station Antennas," in ***IEEE Transactions on Wireless Communications***, vol. 9, no. 11, pp. 3590-3600, November 2010.

[28] H. Q. Ngo, E. G. Larsson and T. L. Marzetta, "Energy and Spectral Efficiency of Very Large Multiuser MIMO Systems," in ***IEEE Transactions on Communications***, vol. 61, no. 4, pp. 1436-1449, April 2013.

[29] Gimenez, Sonia, et al. "Performance Evaluation of Analog Beamforming with Hardware Impairments for mmW Massive MIMO Communication in an Urban Scenario." *Sensors* 16.10 (2016): 1555.

[30] K. Shen and W. Yu, "Distributed Pricing-Based User Association for Downlink Heterogeneous Cellular Networks," in ***IEEE Journal on Selected Areas in Communications***, vol. 32, no. 6, pp. 1100-1113, June 2014.

[31] “M.2135 Guidelines for evaluation of radio interface technologies for IMT-advanced,” ITU Radiocommunications Sector, December 2009.

[32] E. Aryafar, A. Keshavarz-Haddad, M. Wang and M. Chiang, "RAT selection games in HetNets," ***2013 Proceedings IEEE INFOCOM***, Turin, 2013, pp. 998-1006.